Animal Biotelemetry

RESEARCH

Open Access

Performance of a fine-scale acoustic positioning system for monitoring temperate fish behavior in relation to offshore marine developments

Oliver N. Shipley[1*], Ashley Nicoll[1], Robert M. Cerrato[1], Keith J. Dunton[2], Bradley J. Peterson[1], Matthew Sclafani[1,3], Charles Bangley[4,5], Matthew T. Balazik[6], Matthew Breece[7], Brianna V. Cahill[1], Dewayne A. Fox[8], Benjamin I. Gahagan[9], Jeff Kneebone[10], Farrah Leone[1], Maria Manz[1], Matthew Ogburn[11], William C. Post[12], Brittney Scannell[1] and Michael G. Frisk[1]

Abstract

Rapid global expansion of offshore wind farms, tidal, and wave technologies signifies a new era of renewable energy development. While a promising means to combat the impacts of climate change, such developments necessitate fine-scale monitoring of biological communities to determine impacts associated with construction, operation, and eventual decommission. Here, we evaluate the performance of a gridded, Innovasea Systems, Inc. fine-scale acoustic telemetry positioning system (FSPS, $n = 20$ acoustic receivers) for tracking behaviors of diverse, temperate fish assemblages in relation to a subsea cable route supporting the Ørsted offshore wind development in coastal New York. We examined array performance through positioning error derived from receiver reference transmitters and tracked animals ($n = 260$) comprising 17 species of teleost and elasmobranch. We evaluated the effects of environmental variables (temperature, tilt, noise, and depth), transmitter power, individual movement rates, and receiver loss on horizontal positioning error (HPE) and route mean squared error (RMSE). Across a 16-month deployment period, many positions were derived for Atlantic sturgeon ($n = 2{,}612$), black sea bass ($n = 9{,}175$), clearnose skate ($n = 10{,}306$), summer flounder ($n = 13{,}304$), and little skate ($n = 15{,}186$), suggesting that these species may serve as sentinel candidates for assessing behavioral changes following construction, operation, and decommission. We found that receivers placed at the boundary of the grid exhibited higher HPE and RMSE, however these errors did not significantly change despite large receiver losses (25%). Generalized Linear Models revealed that temperature, noise, tilt, and depth were often significant predictors of HPE and RMSE, however, a substantial amount of variance was not explained by the models (~ 70%). Average movement rates ranged from 1.1 m s^{-1} (common thresher shark) to 0.03 m s^{-1} (little skate and summer flounder) but had minimal effects on positioning error. Finally, we observed that higher transmitter powers (158 dB) may lead to higher and more variable HPE values. Overall, these findings provide new insight into the drivers of FSPS array performance and illustrate their broad utility for monitoring fish behavior associated with offshore marine developments.

Keywords Passive acoustic telemetry, Biotelemetry, Elasmobranch, Teleost, Renewable energy, Animal movement

*Correspondence:
Oliver N. Shipley
oliver.shipley@stonybrook.edu
Full list of author information is available at the end of the article

Background

The growing impacts of climate change have demanded urgent global expansion of renewable energy solutions [35, 41], which in marine environments, has led to substantial increases in offshore developments (ODs) supporting wind farm [15], wave energy [13], and tidal energy technologies [31]. These developments necessitate large-scale industrial use of the marine environment and are a relatively new addition to existing human activities, such as dredging, cable installation, shellfish harvesting, finfish farming, and trawling, among others. As societal use of the marine environment increases to meet an expanding human need for marine-based resources, innovative and effective methods must be developed to measure the potential impacts on local species and ecosystems.

As new developments increase, so do concerns over the ecological impacts associated with various phases of construction, operation, and decommissioning that could threaten biodiversity and ecosystem function [47, 55]. These include, but are not limited to, sediment disruption, toxicant release, changes to local hydrodynamic regimes, trophic restructuring [55], change to existing habitat types (e.g., the addition of hard structures), alteration of biogeochemical processes and attraction/dispersion of species to altered habitats [2, 3]. In addition, the output of electromagnetic fields (EMFs) by subsea power cables on marine organisms represents a leading concern associated with many ODs, particularly wind farms [15, 18]. Given the growing distance of many ODs from shore and associated shifts from alternating current (AC) to direct current (DC) power transmission, it is expected that EMFs from subsea cables will increase in the coming decades [18]. While there is limited information on the effects of EMFs, they can potentially alter the behavior and movement of organisms, especially electrosensitive fishes and cetaceans [18], some of which are already of conservation concern [28, 37]. Mitigating these potential impacts requires nuanced monitoring techniques that yield detailed information on residency and behavioral patterns of marine organisms at high spatial resolutions, which poses a challenge in dynamic marine environments.

Passive acoustic telemetry systems have long provided a solution for monitoring occurrence and behaviors of marine organisms [19, 24] and such techniques have been readily integrated into environmental monitoring assessments related to ODs [38–40]. The capacity of acoustic telemetry monitoring systems to evaluate behavioral responses has greatly expanded in recent years, owing to the development and implementation of fine-scale positioning systems [25, 36]. Many studies have utilized the Fine Scale Positioning System (FSPS) from Innovasea Systems, Inc. (Nova Scotia, Canada), formerly Vemco Positioning System (VPS). The FSPS uses the time difference of arrival (TDOA, 57) derived from acoustic transmissions at multiple (i.e., three or more) receivers to accurately position tagged animals in space and time [12, 42]. As such, these systems can be used to ask previously unreachable questions regarding fine-scale behavior and species interactions that cannot be ascertained using other biotelemetry techniques [8, 25, 36, 51]. In fact, there have been several direct applications of an FSPS to monitor behavioral changes of fish relative to seismic surveys [52] and piledriving [53] associated with the development of offshore windfarms.

Despite potential of the FSPS, their effective implementation across expansive environments, such as the coastal ocean, requires detailed spatial planning that maximizes ecological information collected from target species [4, 12, 36]. This is in part, because highly expansive arrays would require hundreds of receivers (e.g., [4]) and therefore be too costly to implement in most environmental monitoring scenarios. Dynamic, temperate environments pose additional challenges due to the seasonality of species occurrence and harsh environmental conditions that can impact the performance of acoustic systems. For example, factors such as turbidity, tides, temperature swings, and high wave action may all reduce detection efficiency and increase gear loss [21, 26, 27, 32, 40] in addition to human activities, such as commercial fisheries, dredging, and installation of power cables (reviewed by [36]). Finally, given the diversity of species life-history strategies associated with temperate assemblages, it remains unclear how FSPS arrays may perform across taxa. Several recent review papers have outlined best practices for FSPS design and techniques for maximizing data quality [25, 36], however, these compilations highlight an empirical lack of performance validation in temperate nearshore environments.

Here, we present results from an FSPS deployed around a subsea power cable associated with the Ørsted South Fork Wind Farm (ØSFWF), a wind energy development area off southern Long Island, New York. Given the few applications of an FSPS to study animal behavior in temperate marine environments, our goal was to validate the array's ability to determine fine-scale behaviors across fishes with diverse life-histories (e.g., low to high mobility). Specifically, we compared how positioning error varied relative to a suite of environmental variables (e.g., temperature, noise, tilt, and depth), fish movement rates, transmitter power, and after losing 25% of the receivers. These findings provide strategic guidance to help refine fine-scale monitoring of diverse, temperate fish assemblages related to proposed construction and operation of human activities in ocean environments.

Methods

Study location

Research was conducted between August 2021 and December 2022 in coastal waters off southern Long Island, New York. The Ørsted South Fork Wind Farm (ØSFWF) is a 130 MW offshore wind project in development 56 km east of Montauk Point and is expected to be New York's first operational offshore wind farm. Ørsted and Eversource were awarded the contract to construct this farm by the Long Island Power Authority (LIPA) in 2017, and it was anticipated to begin operation in late 2023 or early 2024. The farm's 12 turbines are projected to generate sufficient clean energy to power 70,000 homes. This power will be connected to the Town of East Hampton, NY's local grid via an underground transmission cable (the South Fork Export Cable (SFEC), Fig. 1A).

Acoustic array design, deployment, and maintenance

The FSPS was stationed to overlap the central cable approach and comprised a grid (4 rows × 5 columns) of 20 VR2AR acoustic receivers (Innovasea Systems Inc., Nova Scotia, Canada) deployed at depths between 11 and 18 m (Fig. 1A, B). We note that during deployments, some receivers may drift leading to increases in the measured depth by each receiver. The subsea cable (Fig. 1A, B) was inactive during the entire study period. Data are presented from three deployment periods (August 2021–May 2022; May 2022–August 2022; August 2022–December 2022), with the time between receiver downloads ranging from ~ 104 days to ~ 248 days. During the second deployment period, seven receivers were lost, two of which were returned by commercial fishers and incorporated into the dataset. The remaining five were associated with entire data losses. This provided a valuable opportunity to assess array performance after a 'natural' 25% receiver loss, given that no losses occurred during the first or third deployment periods.

Previous work has suggested that a 600 m radius is likely to provide reliable detection information [30], even in 'noisy' environments [21]. Here, each receiver was placed at a conservative distance of ~ 350 m apart and equipped with onboard transmitters (herein, 'reference transmitters', transmission interval = 540–660 s) that were detected by adjacent receivers to provide two-dimensional positioning. For the first deployment period, receivers were attached to a 181 kg square concrete mooring by 3 m of 9.5 mm chain. Buoyancy was achieved by attaching the receiver to two 28 cm trawl balls (5 kg flotation) via 11 mm diameter rope (Appendix S1, Fig. S1A). During the second and third deployment periods, receivers were secured to 68.0 kg steel mooring anchors using a VR2AR-PUB mooring tether comprising 2 m of 9.5 mm diameter dyneema rope with a nylon mooring eye and a tygon tubing chafe guard. Two 28 cm pop-up buoys were secured approximately 1 m above the receiver nipple using a 6.3 mm molded urethane rope and a 7.9 mm galvanized anchor bolt shackle (Appendix S1, Fig. S1B). Receivers were retrieved using an acoustic release command initiated by a VR100 hydrophone. During maintenance, all receivers were downloaded, reset, and redeployed in the same target location with the same mooring.

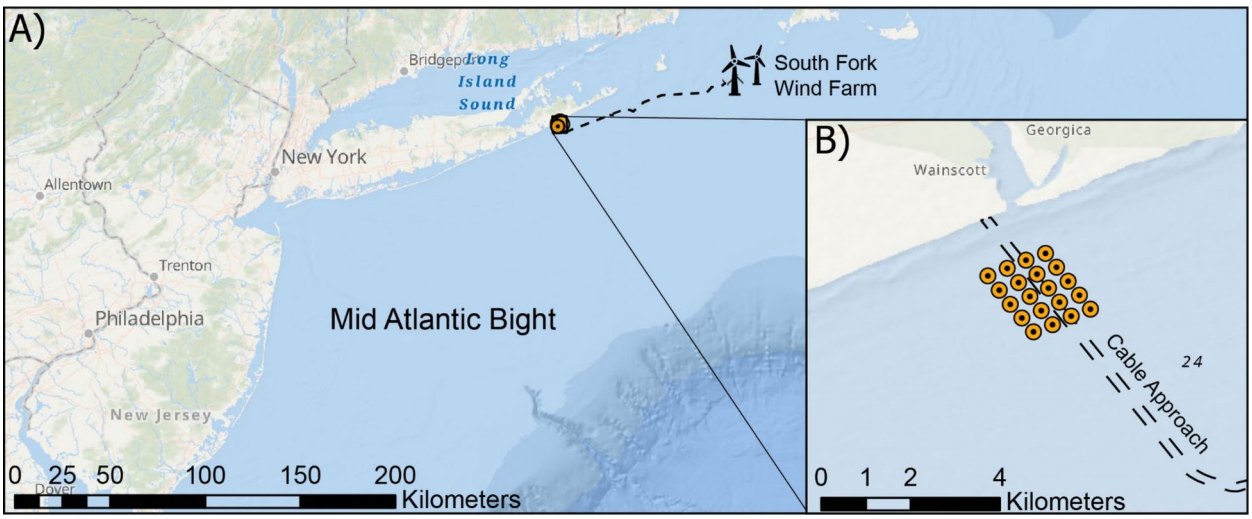

Fig. 1 **A** Location of the acoustic array, cable approach, and South Fork Wind Farm (indicated by the turbine icon), relative to the broader New York Bight and NW Atlantic Ocean and (**B**) the fine scale positioning system (FSPS) comprises an array of 20 (4 rows × 5 columns) acoustic receivers directly intercepting the cable approach to shore

Fish capture and tagging

Fish ($n = 201$) were captured using various techniques, including benthic otter trawl, beam trawl, and rod and reel angling. For teleost fishes and skates, individuals were brought aboard the research vessel, and all were measured for fork and total length (mm) before being placed into a holding tank with flowing seawater and anesthesia (clove oil, 3.8 g L^{-1}). Acoustic transmitters were surgically implanted in the peritoneal cavity, with the incision sutured with 2–3 interrupted stitches. Individuals were then placed back into the holding tank to recover from anesthesia and released. For sharks captured via rod and reel angling, workup procedures followed that of Shipley et al. [44]. Briefly, individuals were secured alongside the research vessel, and precaudal length, fork length, and total length measurements were taken. Individuals were then placed into tonic immobility and tagged using the same approach as for teleost fishes and skates.

Larger individuals (i.e., sharks and Atlantic sturgeon) were implanted with V16 ultrasonic transmitters (69 kHz, high-power output = 158 dB re 1 µPa at 1 m, random transmitter delay = 120 s, life-span = 3650 d, Innovasea Systems Inc.), whereas medium to small bodied individuals (i.e., those for which the peritoneal cavity was too small to implant a V16) were tagged with either a V13 (69 kHz, low-power output = 147 dB re 1 µPa at 1 m, random transmitter delay = 180 s, life-span = 1825 d) or a V9 transmitter (69 kHz, low-power output = 146 dB re 1 µPa at 1 m, random transmitter delay = 120 s, life-span = 650 d). Striped bass (*Morone saxatilis*) were tagged with V13AP transmitters (69 kHz, lower-power output = 147 dB re 1 µPa at 1 m, random transmitter delay = 180 s, lifespan = 1285 d); however, we do not report the collected acceleration or pressure data in this study. It must be noted that information related to specific tag powers was not provided under the collaborative data use agreement (see below), so subsequent analyses integrating tag power were undertaken on a subset of the total data.

Collaborative data use

Detection information for additional telemetered individuals ($n = 59$) was acquired through data sharing agreements. Initial data collection was achieved through the Atlantic Cooperative Telemetry Network's MATOS data portal and direct contact by individual researchers or Innovasea Systems, Inc.. Twenty-three researchers/institutions participated and decided to be acknowledged or included as a co-author. Further information on researchers/institutions is provided in the acknowledgments section.

Data processing and statistical analysis

Calculation of animal positions and positioning error

After each download period, detection data were sent to Innovasea Systems, Inc. and processed using the time distance of arrival (TDOA) hyperbolic positioning algorithm [57]. Here, position estimates were based on TDOA for each transmission at a minimum of three and a maximum of six receivers with synchronized clocks to reduce positioning error [4]. Here, we report weight-averaged positions with associated error sensitivity inferred from both animal and receiver reference transmitters. Error metrics include horizontal positioning error sensitivity of a synthesized position [57], detection time error for a given position defined by the root mean squared error (RMSE, milliseconds), and for reference transmitters, the horizontal positioning error (HPE_m). HPE is a unitless metric that may be influenced by the effects of the geometry of transmitter positions and detecting receivers and is commonly utilized when fixed transmitter/receiver locations are unknown [57], [58]. While HPE values are array-dependent, previous work has suggested filtering positions with HPE < 15 can provide a 33% decrease in positioning error [42]. RMSE refers to a time-based positioning error due to multipath signals, such as signal reflection or refraction [57]. Combined, HPE and RMSE can validate the array performance under different scenarios (e.g., after receiver losses, reviewed by [36]).

The array design uses receiver reference transmitters at fixed locations to provide a complementary measure of horizontal positioning error in units of distance (HPE_m). HPE_m represents the distance between a calculated position and the known position of the reference transmitter [57, 58]. The receiver reference transmitters produce a V9 (69 kHz, low-power output = 160 dB re 1 µPa at 1 m, random transmitter delay = 120 s, lifespan = 650 d) acoustic transmission similar to transmitters implanted into animals. Aggregated estimates of HPE_m were calculated for all interior (internal receivers, highest potential for positioning accuracy) and boundary (edge receivers, lowest potential for positioning accuracy) receivers.

Effects of receiver loss on HPE and RMSE

The effect of significant receiver losses on HPE and RMSE was compared for each receiver location in the array and relative to two download periods comprising no receiver loss, using data from reference transmitters. Seven receivers were lost in the second deployment period (May 2022–August 2022). However, two were returned and incorporated into the dataset for the time that they remained in the correct deployment locations. This resulted in a 25% loss of receivers in the array for that deployment period. HPE_m between boundary (i.e., those on the outside, $n = 14$) and interior (i.e., those on

the inside, $n=6$) receivers for each download period were compared using 2.5th, 50th, and 97.5th percentiles. To investigate the effects of receiver loss further, we determined spatial variation of mean daily HPE and RMSE associated with individual animal positions. These were visually compared across the three deployment periods.

Environmental drivers of HPE and RMSE from receiver reference transmitters

The VR2AR receivers provide continuous estimates of several environmental parameters, including temperature (°C), tilt (°), depth (m), and noise (mV). We therefore determined their relative effects on both HPE and RMSE using positions derived from the receiver reference transmitters. First, we averaged HPE, RMSE, temperature, noise, tilt, and depth for each hour ($n=11{,}488$ total measurements across the entire deployment time series), then took 300 random draws to remove temporal autocorrelation. We used Generalized Linear Models (GLMs) to determine relationships between HPE and RMSE and the environmental variables all of which were treated as fixed effects. Because HPE and RMSE did not conform to a Gaussian distribution, error was modelled using a Tweedie family and log link function. Variance power was estimated using maximum likelihood through the *tweedie.profile* function in the R package *tweedie* [11]. We then calculated variance inflation factors (VIFs) to examine the combined collinearity of the environmental predictors. Model fit was assessed through visual inspection of QQ plots and determination of R^2 defined as 1-deviance/null deviance.

Effect of tag power and rate of movement on HPE and RMSE from animal transmitters

We assessed the effects of transmitter power (146, 147, and 158, dB re 1 µPa at 1 m) and average rate of movement (ROM, m s^{-1}) derived for each tagged individual on HPE and RMSE. Because tag powers were not provided by external collaborators, the following analyses are conducted on a smaller subset of tagged animals managed by the project PIs, comprising 201 individuals from 17 species (see Appendix S1, Table S1). Here, we used positions collected across the entire deployment duration to maximize the number of positions available for statistical resampling (see below).

Individual ROM was calculated for all individuals with three or more positions across all download periods following:

$$\mathrm{ROM} = \frac{\sqrt{(x_2 - x_1)^2 + (y_2 - y_1)^2}}{t_2 - t_1}, \quad (1)$$

where x and y are the planar locations of the positioned individual at times 1 and 2, and t is the timestamp of the position at times 1 and 2. The initial dataset included >49,000 average ROM estimates across all individuals (Appendix S1, Table S1). Given that the number of individuals associated with each transmitter power was greatly unbalanced, we took 100 random draws from individuals comprising each tag power. We then adopted the same modelling approach as for the environmental data, including fixed effects of tag power and ROM. Given that the number of individuals comprising each species was highly variable ($n=96$ to $n=1$) and many species were fitted with the same tag power, we did not directly test for the effect of species. However, we report mean (± SE) ROM, HPE, and RMSE values for each species derived from the full dataset (i.e., including positions calculated from collaborator transmitters).

All statistical analyses other than calculation of transmitter positions and error estimates were conducted in R (V4.3.1, R Development Core Team 2023).

Results

Over the study period, 260 individuals spanning 17 species were tracked within the FSPS and provided 53,744 unique positions (Table 1). The greatest number of unique individuals were detected for Atlantic sturgeon ($n=120$), striped bass ($n=33$), and clearnose skate ($n=29$), with the lowest number ($n=1$) detected for the blacktip shark, common thresher shark, spinner shark, white shark, and tautog (Table 1). The highest number of unique positions were estimated for little skate ($n=15{,}186$), summer flounder ($n=13{,}304$), and clearnose skate ($n=10{,}306$), and the lowest number of unique positions were estimated for the white shark ($n=5$), common thresher shark ($n=19$), and tautog ($n=25$) (Table 1). Little skate, black sea bass, and summer flounder exhibited the greatest number of positioning days, with unique positions determined in 79, 41, and 23 days, respectively. Meanwhile, winter skate, the white shark, and tautog had the fewest positioning days and were only detected in a single day (Table 1). Visual inspection of positions revealed that the FSPS was effective in determining different behavioral modes. For example, Atlantic Sturgeon and striped bass appeared to use the array as movement corridors (Fig. 2A–D), whereas clearnose and little skate exhibited higher residency with greater movement tortuosity (Fig. 2E–H).

Effects of receiver loss on HPE and RMSE

Estimates from reference transmitters revealed that HPE and RMSE were highest on the boundary receivers, especially at receivers placed on the grid corners (Fig. 3). However, error ranges across the entire array

Table 1 Summary of tagged animals detected within the FSPS array including size ranges, the total number of unique position estimates, range of days over which unique individuals were detected, the total duration each species was detected, mean HPE and RSME (± SE)

Species	Scientific name	*n*	Total length (cm)	Total positions	Individual position days	Total days positioned	HPE	RMSE
Atlantic Sturgeon	*Acipenser oxyrinchus oxyrinchus*	120	93–233	2,612	1–7	116	15.4 ± 0.7	0.9 ± 0.0
Black Sea Bass	*Centropristis striata*	11	19–39	9,175	1–41	54	8.6 ± 0.1	1.3 ± 0.0
Blacktip Shark	*Carcharhinus limbatus*	1	174	93	4	4	8.9 ± 1.2	0.7 ± 0.1
Clearnose Skate	*Raja eglanteria*	29	23–78	10,306	1–18	44	6.7 ± 0.1	0.5 ± 0.0
Common Thresher Shark	*Alopias vulpinus*	1	190[a]	19	2	2	5.5 ± 0.8	0.7 ± 0.1
Dusky Shark	*Carcharhinus obscuras*	7	96–139	143	1–4	12	26.7 ± 4.1	0.7 ± 0.1
Little Skate	*Leucoraja erinacea*	11	43–47	15,186	1–79	98	4.9 ± 0.0	0.4 ± 0.0
Sandbar Shark	*Carcharhinus plumbeus*	5	128–157	113	1–2	6	22.9 ± 3.3	0.8 ± 0.1
Sand Tiger Shark	*Carcharias taurus*	2	150	50	2	4	15.9 ± 3.1	0.9 ± 0.1
Spinner Shark	*Carcharhinus brevipinna*	1		14	2	2	13.7 ± 7.2	0.9 ± 0.1
Striped Bass	*Morone saxatilis*	33	44–117	289	1–3	25	24.5 ± 3.0	0.7 ± 0.0
Summer Flounder	*Paralichthys dentatus*	12	34–54	13,304	1–23	39	4.9 ± 0.0	0.4 ± 0.0
Tautog	*Tautoga onitis*	1	34	25	1	1	14.3 ± 4.0	0.5 ± 0.1
Weakfish	*Cynoscion regalis*	7	28–51	200	1–2	3	15.0 ± 2.0	0.7 ± 0.0
White Shark	*Carcharodon carcharias*	1	183	5	1	12	45.0 ± 6.8	0.1 ± 0.1
Winter Flounder	*Pseudopleuronectes americanus*	10	31–43	220	1–2	6	6.0 ± 0.6	0.2 ± 0.0
Winter Skate	*Leucoraja ocellata*	8	71–92	136	1	90	6.4 ± 0.4	0.3 ± 0.0

Note that tag powers were not reported under the collaborative data sharing agreement, so are only available for a subset of the total data (see Table S1)

[a] Measured fork length

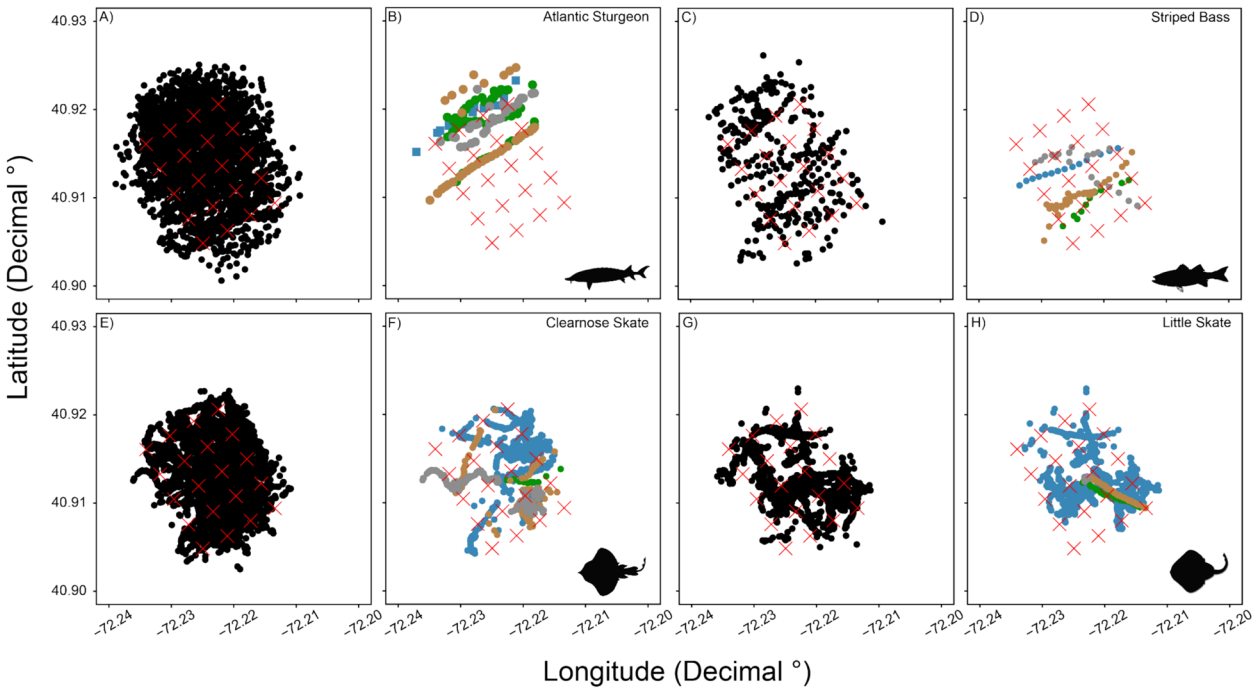

Fig. 2 Fine scale positions of Atlantic sturgeon (**A**, **B**), striped bass (**C**, **D**), clearnose skate (**E**, **F**) and little skate (**G**, **H**), tracked throughout the duration of this study, where colors represent different individuals. Left panels (**A**, **C**, **E**, **G**) represent all positions and right panels (**B**, **D**, **F**, **H**) are positions from four different individuals highlighting transient (top panels) versus resident (bottom panels) behaviors

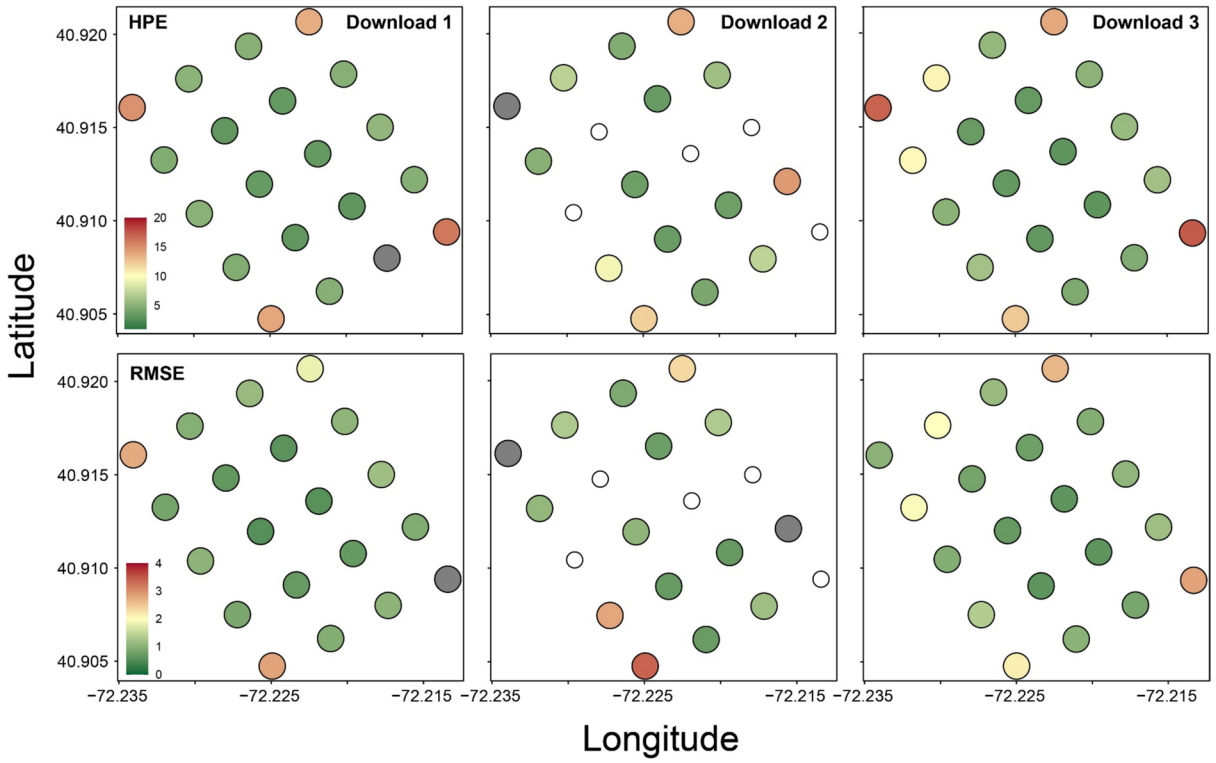

Fig. 3 HPE and RMSE across three deployment periods within the FSPS as derived from receiver reference transmitters. Open circles represent receivers lost during the second deployment period. To allow for an effective color ramp, HPE values from 0 to 20 and RMSE values from 0 to 4 are shown, the upper limit for both HPE and RMSE are ~ 96th percentiles

remained low, with > 77% of total HPE estimates falling below 10 and > 93% of total RMSE estimates falling below 5 across all downloads. Following a 25% receiver loss, median HPE and RMSE derived from the internal reference transmitters increased from 3.6 pre-loss to 5.7 post-loss for HPE and 0.9 to 1.0 for RMSE (Figs. 3, 4A). When converted to HPE_m and categorized by receiver position, this resulted in a change of 1.0–1.3 m for the boundary receivers, and 0–0.1 m for the internal receivers, with larger changes only evident in the 97.5th percentiles (Table 2). For tracked animals, we also observed increases in the median daily HPE (6.4–7.6) and a small decline in RMSE (0.8–0.7) in mid-June when five receivers were displaced across seven days (Fig. 4B). However, there was little change in the spatial variation of HPE and RMSE across the array (Fig. 5).

Environmental drivers of HPE and RMSE from receiver reference transmitters

Generalized Linear Models revealed significant positive effects of temperature, noise, and depth, and a negative effect of tilt on HPE (Table 3, Appendix S2 Fig. S3). For RMSE, there were significant, positive effects of noise and depth, and a negative effect of tilt (Table 3, Appendix S1, Fig. S4). It must be noted that visual inspection of QQ plots and model predictions revealed high residual error and statistical leverage at higher temperatures and depths, and lower noise and tilt for both HPE (Appendix S2, Fig. S3) and RMSE (Appendix S2, Fig. S4). Models identified a considerable amount of unexplained variance (70%) suggesting that the environmental variables were relatively poor predictors of positioning error. Inspection of variance inflation factors suggested that combined collinearity was not likely to result in overfitting for either HPE or RMSE as values did not exceed 2.5 (Fig. S5).

Effects of movement rate and tag power on HPE and RMSE from animal transmitters

Average ROM was highest for the common thresher shark (1.1 ± 0.1 m s^{-1}), blacktip shark (0.8 ± 0.0 m s^{-1}), and spinner shark (0.7 ± 0.1 m s^{-1}), and lowest for little skate (0.03 ± 0.0 m s^{-1}), summer flounder (0.03 ± 0.0 m s^{-1}), and black sea bass (0.04 ± 0.0 m s^{-1}) (Fig. 5A). At the species level, mean HPE estimates were highest for the white shark (45.0 ± 6.8), dusky shark (26.7 ± 4.1) and striped bass (24.5 ± 3.0), and lowest for little skate (4.9 ± 0.0), summer flounder (4.9 ± 0.0), and the common thresher shark (5.5 ± 0.8) (Fig. 5B). Estimates of RMSE did not

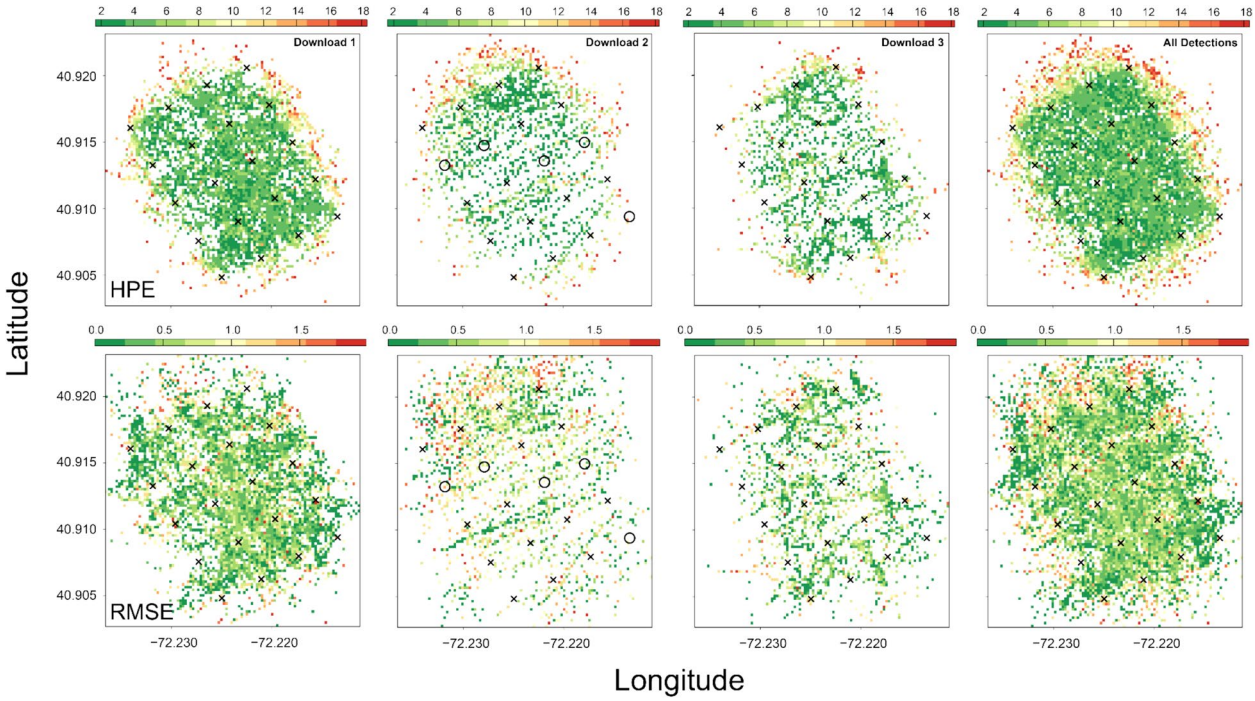

Fig. 4 Mean HPE and RMSE for individual animal positions across the FSPS. Panels represent spatial variation in HPE (top panels) and RMSE (bottom panels) for each deployment period and all positions combined. Black X's indicate active receivers and open circles reflect losses

Table 2 Summary of 2.5th, 50th, and 97.5th percentiles for HPE_m (m) from internal reference transmitters associated with boundary ($n=14$) and internal ($n=6$) receivers

Deployment period	Array position	2.5%	50%	97.5%
August 2021–May 2022	Boundary	0.3	1.8	15.2
	Interior	0.1	0.7	4.2
May 2022–August 2022	Boundary	0.2	2.8	20.7
	Interior	0.2	0.8	4.1
August 2022–December 2022	Boundary	0.3	1.5	11.6
	Interior	0.2	0.7	3.7
All	Boundary	0.3	1.8	15.8
	Interior	0.1	0.7	4.1

align with HPE across species, and estimates were highest for black sea bass (1.3 ± 0.0), the spinner shark (0.9 ± 0.1), and sand tiger shark (0.9 ± 0.1), and lowest for the white shark (0.1 ± 0.1), winter flounder (0.2 ± 0.0), and winter skate (0.3 ± 0.0) (Fig. 5C).

For HPE, GLMs revealed positive effects of 158 dB transmitter power relative to 146 dB and 147 dB, and a significant negative effect of ROM (Table 4, Appendix S2, Fig. S6). There was particularly high residual error at high HPE values, driven by tags transmitting at 158 dB (Appendix S2, Fig. S5). For RMSE, no statistically significant effects were observed (Table 4). However, inspection of QQ plots and R^2 values ($R^2=0.03$) suggested a poor model fit with the selected predictors providing negligible predictive power (Table 4, Appendix S2, Fig. S6).

Discussion

The global threat of climate change has led to rapid development and implementation of technology to harness renewable energy. In ocean environments, much of this relates to the development and production of wind-powered energy, however it is likely that other forms of renewable energy, such as wave and tidal technologies will continue to be explored. These developments all have the potential to alter physical, chemical, and biological features of the marine environment and impact human activities such as fishing. In other areas of the world, such as the North Sea, fine scale positioning systems (FSPS) have already begun to reveal changes to fish behavior associated with offshore wind activities, such as seismic surveys [51, 52]. It is expected that these effects are broadly applicable. Considering that the continental US represents one of the fastest growing offshore wind development areas in the world [9], a vital need exists to monitor the expanding industry and determine any impacts (positive or negative) on living marine resources. This is an important component of responsible development in the marine environment.

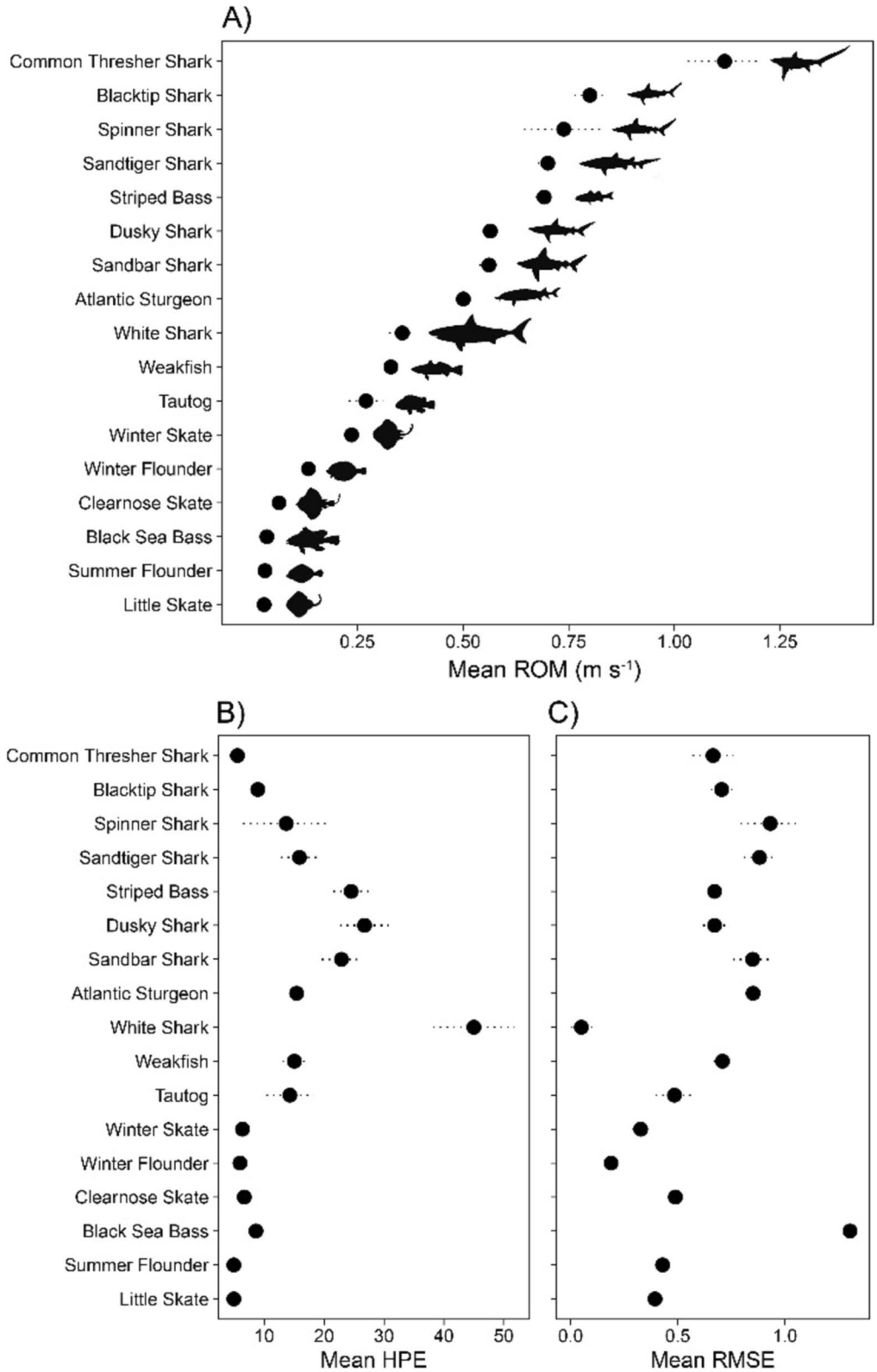

Fig. 5 **A** Mean (± SE) rate of movement (ROM, m s^{-1}) calculated from 2D positions within the FSPS. Species are ordered from highest to lowest average ROM estimates. **B** Mean HPE and (**C**) mean RMSE (± SE) for each species ordered by ROM

Table 3 Summary statistics from Generalized Linear Models assessing the effects of temperature (°C), noise (mV), tilt (°), and depth (m) on HPE and RMSE. Values are model coefficients (SE). Models were derived from positions and error estimated from internal receiver reference transmitters. Environmental data were measured using the VR2AR receivers

Model	Variance Power	Intercept	Temperature	Noise	Tilt	Depth	R^2
HPE ~ temp + noise + tilt + depth	5	0.435 (0.194)*	0.015 (0.003)***	0.001 (0.000)**	-0.018 (0.006)**	0.090 (0.016)***	0.30
HPE ~ temp + noise + tilt + depth	5	− 1.875 (0.261)***	0.006 (0.004)	0.001 (0.000)*	− 0.037 (0.008)***	0.162 (0.022)***	0.22

* Refers to α where * = 0.05, ** = 0.01, ***0.001

Table 4 Summary statistics from Generalized Linear Models assessing the effects of rate of movement (ROM, m s^{-1}) and transmitter power on HPE and RMSE. Values are model coefficients (SE). Models were derived from positions and error estimated from animal transmitters

Model	Variance Power	Intercept	ROM	147 dB	158 dB	R^2
HPE ~ ROM + transmitter power	2.5	1.866 (0.104)***	− 2.566 (0.811)**	-0.1401 (0.137)	2.5771 (0.484)***	0.36
RMSE ~ ROM + transmitter power	2.5	− 0.465 (0.134)***	− 0.4657 (0.966)	− 0.352 (0.190)	0.435 (0.549)	0.03

* Refers to α where * = 0.05, ** = 0.01, ***0.001

Our findings suggest that a relatively localized FSPS can effectively monitor fine-scale behaviors across a diversity of nearshore marine fishes at sub-meter resolution. The performance capacity of the FSPS to accurately position animals (inferred through RMSE and HPE) responded marginally to environmental variation, species life-history diversity (i.e., rate of movement), and transmitter power. Further, we observed small increases in positioning error following a significant receiver loss, which was largely localized to boundary receivers situated on the edge of the gridded array configuration. Collectively, these findings highlight the potential of a small-scale FSPS for monitoring diverse fish behaviors in highly dynamic, temperate environments, such as the northeast US coast. Similar approaches could serve as effective monitoring tools to trace impacts to ecological interactions following the development of offshore structures, such as wind farms, for a wide variety of questions, including understanding the impacts of electromagnetic fields (EMFs).

Impacts of receiver loss on RMSE and HPE

Temperate nearshore environments pose many challenges for maintaining acoustic telemetry arrays due to seasonal effects on detection efficiency (see [46]), wave action through intense storm events, anthropogenic activities such as fishing with bottom-tending gear (e.g., trawl nets and dredges), and the migratory nature of many temperate fish assemblages. In this study, we ascertained how receiver loss impacted positioning error within a gridded FSPS. With an array of twenty functioning receivers (i.e., 100%), the highest positioning error derived from both internal receiver reference transmitters and tracked animals occurred along the array boundaries. However, these estimates were extremely low. For example, median HPE_m values for internal and boundary receivers were 0.8 m and 1.8 m, respectively. This spatial disparity was expected and driven by the lower number of receivers available to ascertain positions when an individual moves beyond the array boundary (Smith 57) [36]. However, the array's central regions yielded consistently low RMSE and HPE throughout the entire deployment period, which also appeared insensitive to seasonality given that deployment periods covered over a year of continuous monitoring. During the second deployment period, the array experienced a significant loss of receivers, which were permanently removed for the remainder of the deployment period. Despite high losses, we did not observe substantial changes in either RMSE or HPE, especially within the central portions of the array. These findings support observations by van der Knaap et al. [51, 52], who found that removing single receivers from circular (= 12.5% loss) and triangular (= 10% loss) array configurations reduced the total number of positions, but resulted in only small increases to HPE (on average < 1), regardless of the specific receiver position. This suggests that multiple receiver configurations may be relatively robust to receiver losses ranging from 10 to 25%, but effects on HPE are likely to be spatially variable. If receiver losses do occur, filtering positions using the average RMSE and HPE values prior to the removal event will ensure negligible losses in array performance and associated ecological inferences.

Environmental drivers of HPE and RMSE

We used receiver reference transmitters to determine the relative impacts of environmental variation on HPE and RMSE. Both types of error increased gradually with temperature, noise, and depth, and decreased with tilt. However, in both models, less than a third of the total variance could be explained by the selected predictors. More notable was the observed increase in residual error at high temperature and depth and low noise and tilt values, suggesting potential effects on positioning error variability. Despite these observations, HPE and RMSE values fell mostly below 10 and 5 across the entire deployment duration, respectively, suggesting only marginal impacts of the measured environmental predictors. Complexity between environmental variation and both positioning error and probability has been established across freshwater, estuarine, and marine environments elsewhere [4, 46]. For example, warmer temperatures were associated with higher HPE_m values derived from static reference transmitters deployed throughout arrays in coastal San Diego and the San Francisco estuary, CA [46]. Here, the authors attributed this relationship to differences between the average water temperatures used to estimate the speed of sound and subsequent triangulation, relative to the actual measured temperatures within an array. Greater disparity between the actual versus average estimates used in these post-processing equations could explain the positive relationships observed in the current study and the higher residual error associated with higher temperatures. We also observed weak positive relationships between HPE and RMSE and noise. This was not surprising, however, because the FSPS is stationed in an area associated with high boat activity, wave action, with additional biological sound potentially driven by marine organisms such as toadfish and eels [59]. However, noise estimates were rarely at levels expected to impact positioning efficiency (> 300 mV, [50]). Greater study of the ambient marine soundscape would help to further contextualize the ultimate drivers of noise, and those most likely to mask acoustic signals associated with reference and animal transmitters.

The observed relationships between positioning error and tilt and depth are challenging to explain. Negative relationships between tilt and HPE and RMSE may be inaccurate, due to high statistical leverage and low sample sizes at greater tilt values. The higher errors associated with greater depths could be attributed to thermal stratification and the position of the thermocline (per [4]) or the distance over which animals are positioned. However, further work is required to contextualize these relationships for our study system and others. Overall, we conclude that the relationships between HPE and RMSE and environmental variables are dynamic and complex. We strongly recommend that future studies continue to establish these relationships using reference transmitters deployed within the FSPS given that relationships are likely to be regionally variable.

Impacts of transmitter power and ROM on HPE and RMSE

We accurately determined fine-scale positions from 17 fish species of diverse life histories, including highly migratory flatfish, sturgeon, and elasmobranchs. Several species, such as clearnose skate, little skate, black sea bass, and summer flounder, exhibited extremely high residency (> 9,000 unique positions) and could therefore serve as important sentinels for determining behavioral modifications following development activities. Visual inspection of animal positions for clearnose skate and Atlantic sturgeon highlights potential for categorizing resident versus more transient behavior. For skates and sturgeon that use specialized electrosensory structures for locating prey buried within the benthos, this is a particularly promising observation given the potential for EMF-induced disruptions to foraging [17] and migration [22]. There remain trade-offs, however, as increasing the number of tagged individuals exhibiting high residency within a small area may increase signal collisions, which can increase positioning error [4, 36].

Though black sea bass were consistently positioned within the FSPS (> 9,000 positions from 11 individuals), this species exhibited a notably higher RMSE (1.3 ± 0.0) relative to the rest of the monitored assemblage (≤ 0.9). High RMSE values could reflect an association with hard structures on the benthos, which are known to increase multipath signals [36]. Considering that many offshore developments require the introduction of hard, resistant substrate and complex structures, positioning fishes that commonly associate with structures could prove challenging, at least at the resolution necessary to quantify discrete behaviors. In these cases, measuring additional parameters, such as depth and acceleration, may improve behavioral inferences if positioning error is high and somewhat unreliable. For example, recent work in the Belwind/Nobelwind offshore wind farm applied acceleration transmitters to Atlantic cod (*Gadus morhua*) in an FSPS and were able to infer declining activity and interruptions to diurnal activity rhythms associated with experimental seismic surveys [51, 52]. However, using acceleration transmitters in an acoustic context remains in its infancy despite showing clear promise for identifying behavioral activity rhythms (see [25] and references therein).

Positions were derived for coastal shark species, several of which typically associate with offshore pelagic environments (the white shark and common thresher shark, [23, 45]). While positioning errors were comparable

to other species , the total number of derived positions was comparatively low (435 unique positions across seven species), suggesting that effective monitoring of highly migratory sharks will require increased tagging efforts (including transmitters with faster transmission rates) and array expansion. The latter could be facilitated through coordination with additional acoustic receiver arrays and extending monitoring over several years. This finding highlights the challenges associated with monitoring core habitat use in highly migratory sharks more generally, especially in regions such as coastal New York, where residency is seasonal [1, 7, 43, 44]. Therefore, establishing known home ranges for mobile predators more generally is needed to improve the efficacy of behavioral information collected through a FSPS. These research efforts are of high priority, given the declining conservation status of many species [33, 34], their observed sensitivities to climactic change [5, 16], and the propensity for offshore developments to disturb key behaviors such as migration [14].

Generalized Linear Models revealed that HPE estimates were larger and more variable for animals tagged with 158 dB transmitters. This could be attributed to higher power transmitters being positioned from greater distances or reduced signal reflection associated with lower power transmitters [54]. These findings suggest that the use of lower power transmitters may be favorable for optimizing behavioral data yielded through the FSPS, especially for resident species that displayed high tortuosity, such as clearnose skate and little skate. We also observed significant, negative relationships between HPE and rate of movement, but the overall change was low suggesting a minimal impact. For RMSE, models did not perform well and explained a negligible amount of the total variance ($R^2 = 0.03$) and therefore precluded robust evaluation of RMSE predictors.

Additional considerations

Our results provide promising support for the use of a FSPS to track behavioral changes in many species of temperate marine fishes in relation to the development of offshore structures. However, additional sources of noise can affect array performance and we were unable effectly to quantify these in this study. For example, the development of major offshore activities, such as wind farms, introduces a substantial amount of additional noise into the marine environment through increases in seismic (i.e., pile driving, [36]) and boat activity [6] and operation of turbines [49]. This is additive relative to the noise associated with tides, high wave action from storms, and animals, which we assume is captured in receiver measurements [10, 26, 36, 48, 56]. Second, offshore development activities can introduce large amounts of sediment, scour, debris, artificial growth, and air bubbles into the water column, all of which are known to significantly reduce the detection range and associated positioning accuracy [6, 36]. These impacts could be somewhat mitigated by reducing the distance between receivers within the FSP and calls for further experimental work that explores the drivers of detection range variability. Combined, these factors can significantly reduce array performance, suggesting that telemetry-based approaches may benefit from being coupled with additional survey techniques that can trace changes in ecological interactions and assemblage structure, such as environmental DNA, fisheries independent monitoring surveys, and biochemical tracers (see [20, 29]).

Conclusions

While we acknowledge the challenges associated with deploying the FSPS in temperate marine environments they hold great promise for monitoring behavioral impacts associated with offshore marine developments. We highlight that for many species, a substantial number of accurate positions (< 1 m) can be derived and used to identify unique behavioral modes. A greater number of accurate positions (and therefore behaviors) are likely to be yielded from species that exhibit high residency, such as skates and flounders. We find some spatial variation in positioning error, suggesting that boundary receivers, particularly those at the corners of gridded arrays, may exhibit slightly higher positioning error relative to more central receivers. However, moderate loss of the FSPS did not dramatically increase positioning error in any location. Given the rapid development of offshore structures, especially offshore wind farms in temperate marine environments, the FSPS may be an effective tool for nuanced monitoring of ecological changes at various development stages.

Abbreviations

ØSFWF	Ørsted South Fork Wind Farm
NW	Northwest
FSPS	Fine scale positioning system
TDOA	Time distance of arrival
HPE	Horizontal positioning error
RMSE	Route mean squared error

Supplementary Information

The online version contains supplementary material available at https://doi.org/10.1186/s40317-024-00386-x.

Supplementary Material 1.

Acknowledgements

The authors would like to acknowledge E. Hilton, P. McGrath, M. Fogg, A. Irvin, J. Zacharias, T. Eigenberger, B. Gagliardi, C. Harter, and C. Paparo. Additionally, the authors would like to thank the staff at Innovasea Systems, Inc. for processing these FSPS data., the Atlantic Cooperative Telemetry Network,

OTN. We thank members of the striped bass program at the Marine Biological Laboratory for their willingness for us to use detections of striped bass that they tagged.

Author contributions
ONS, RMC, KJD, BJP, MS, and MGF conceived the study. ONS, AN, RMC, KJD, BJP, MS, CB, MTB, MB, BVC, DAF, BIG, JK, FL, MM, MO, WCP, BS conducted fieldwork, maintained telemetry arrays, performed fish tagging, and contributed data. ONS and AN conducted statistical analysis. ONS, AN, and MGF wrote the manuscript with significant input from all authors. All authors approved the final version of the manuscript.

Funding
We are grateful for funding provided to Stony Brook University and Monmouth University by ØRSTED. Funding for dusky and spinner shark transmitters deployed by the Smithsonian Environmental Research Center was provided by Aramco Services Company. Funding for acoustic telemetered sharks and finish was provided by the New York State Department of Environmental Conservation to Stony Brook University's Expanded Acoustic Monitoring Project.

Availability of data and materials
The datasets used and/or analyzed during the current study are available from the corresponding author on reasonable request.

Declarations

Ethics approval and consent to participate
This work was carried out under permits from the New York State Department of Environmental Conservation (License to Collect or Possess: Scientific 1110; Endangered/Threatened Species Scientific License 336) and the National Oceanographic and Atmospheric Administration (SHK-LOA-17-08). Atlantic Sturgeon were tagged under National Marine Fisheries Service (NMFS) Endangered Species Permits 16507, 20548, 16422, and 20351. Surgical procedures followed approved SBU Institutional Animal Care and Use Committee approved protocols (#1173245).

Consent for publication
Not applicable.

Competing interests
The authors declare no competing interests.

Author details
[1]School of Marine and Atmospheric Sciences, Stony Brook University, Stony Brook 11794, USA. [2]Department of Biology, Monmouth University, West Long Branch, NJ, USA. [3]Cornell Cooperative Extension-Suffolk Count, 423 Griffing Ave, Riverhead, NY 11901, USA. [4]Department of Biology, Dalhousie University, Halifax, NS, CA, Canada. [5]Department of Mathematics and Statistics, Dalhousie University, Halifax, NS CA, Canada. [6]Rice Rivers Center, Virginia Commonwealth University, PO Box 842030, Richmond, VA 28577, USA. [7]College of Earth Ocean and Environment, University of Delaware, Lewes, DE, USA. [8]Department of Agriculture and Natural Resources, Delaware State University, Dover, DE, USA. [9]Massachusetts Division of Marine Fisheries, 30 Emerson Ave., Gloucester, MA 01930, USA. [10]Anderson Cabot Center for Ocean Life, New England Aquarium, Boston, MA, USA. [11]Fisheries Conservation Lab, Smithsonian Environmental Research Center, Edgewater, MD 21037, USA. [12]South Carolina Department of Natural Resources, Marine Resources Research Institute, PO Box 12559, Charleston, SC 29422, USA.

Received: 1 March 2024 Accepted: 7 October 2024
Published online: 04 December 2024

References

1. Bangley CW, Curtis TH, Secor DH, Latour RJ, Ogburn MB. Identifying important juvenile Dusky Shark habitat in the northwest Atlantic Ocean using acoustic telemetry and spatial modeling. Mar Coastal Fish. 2020;12(5):348–63.
2. Bailey H, Brookes KL, Thompson PM. Assessing environmental impacts of offshore wind farms: lessons learned and recommendations for the future. Aquat Biosyst. 2014;10(1):1–13.
3. Bergström L, Kautsky L, Malm T, Rosenberg R, Wahlberg M, Capetillo NÅ, Wilhelmsson D. Effects of offshore wind farms on marine wildlife—a generalized impact assessment. Environ Res Lett. 2014;9(3): 034012.
4. Binder TR, Holbrook CM, Hayden TA, Krueger CC. Spatial and temporal variation in positioning probability of acoustic telemetry arrays: fine-scale variability and complex interactions. Anim Biotelemetry. 2016;4:1–15.
5. Braun CD, Lezama-Ochoa N, Farchadi N, Arostegui MC, Alexander M, Allyn A, et al. Widespread habitat loss and redistribution of marine top predators in a changing ocean. Sci Adv. 2023;9(32): eadi2718.
6. Brownscombe JW, Lédée EJ, Raby GD, Struthers DP, Gutowsky LF, Nguyen VM, et al. Conducting and interpreting fish telemetry studies: considerations for researchers and resource managers. Rev Fish Biol Fish. 2019;29:369–400.
7. Curtis TH, Metzger G, Fischer C, McBride B, McCallister M, Winn LJ, et al. First insights into the movements of young-of-the-year white sharks (Carcharodon carcharias) in the western North Atlantic Ocean. Sci Rep. 2018;8(1):10794.
8. Dahl KA, Patterson WF III. Movement, home range, and depredation of invasive lionfish revealed by fine-scale acoustic telemetry in the northern Gulf of Mexico. Mar Biol. 2020;167(8):111.
9. DeCastro M, Salvador S, Gómez-Gesteira M, Costoya X, Carvalho D, Sanz-Larruga FJ, Gimeno L. Europe, China and the United States: three different approaches to the development of offshore wind energy. Renew Sustain Energy Rev. 2019;109:55–70.
10. Duarte CM, Chapuis L, Collin SP, Costa DP, Devassy RP, Eguiluz VM, Juanes F. The soundscape of the Anthropocene ocean. Science. 2021;371(6529): eaba4658.
11. Dunn PK. Tweedie: evaluation of Tweedie exponential family models. R package version 2.3. 2022.
12. Espinoza M, Farrugia TJ, Webber DM, Smith F, Lowe CG. Testing a new acoustic telemetry technique to quantify long-term, fine-scale movements of aquatic animals. Fish Res. 2011;108(2–3):364–71.
13. Falcao AFDO. Wave energy utilization: a review of the technologies. Renew Sustain Energy Rev. 2010;14(3):899–918.
14. Farr H, Ruttenberg B, Walter RK, Wang YH, White C. Potential environmental effects of deepwater floating offshore wind energy facilities. Ocean Coast Manage. 2021;207: 105611.
15. Gill AB, Bartlett M, Thomsen F. Potential interactions between diadromous fishes of U.K. conservation importance and the electromagnetic fields and subsea noise from marine renewable energy developments. J Fish Biol. 2012;81:664–95.
16. Hammerschlag N, McDonnell LH, Rider MJ, Street GM, Hazen EL, Natanson LJ, et al. Ocean warming alters the distributional range, migratory timing, and spatial protections of an apex predator, the tiger shark (Galeocerdo cuvier). Global Change Biol. 2022;28(6):1990–2005.
17. Hutchison ZL, Secor DH, Gill AB. The interaction between resource species and electromagnetic fields associated with electricity production by offshore wind farms. Oceanography. 2020;33(4):96–107.
18. Hutchison ZL, Gill AB, Sigray P, He H, King JW. A modelling evaluation of electromagnetic fields emitted by buried subsea power cables and encountered by marine animals: considerations for marine renewable energy development. Renewable Energy. 2021;177:72–81.
19. Hussey NE, Kessel ST, Aarestrup K, Cooke SJ, Cowley PD, Fisk AT, et al. Aquatic animal telemetry: a panoramic window into the underwater world. Science. 2015;348(6240):1255642.
20. Huveneers C, Simpfendorfer CA, Kim S, Semmens JM, Hobday AJ, Pederson H, et al. The influence of environmental parameters on the performance and detection range of acoustic receivers. Methods Ecol Evol. 2016;7(7):825–35.
21. Kessel ST, Cooke SJ, Heupel MR, Hussey NE, Simpfendorfer CA, Vagle S, Fisk AT. A review of detection range testing in aquatic passive acoustic telemetry studies. Rev Fish Biol Fish. 2014;24:199–218.
22. Klimley AP, Putman NF, Keller BA, Noakes D. A call to assess the impacts of electromagnetic fields from subsea cables on the movement ecology of marine migrants. Conserv Sci Pract. 2021;3(7): e436.
23. Kneebone J, Bowlby H, Mello JJ, McCandless CT, Natanson LJ, Gervelis B, et al. Seasonal distribution and habitat use of the common thresher shark

(Alopias vulpinus) in the western North Atlantic Ocean inferred from fishery-dependent data. Fish Bull. 2020;118:399.
24. Lennox RJ, Aarestrup K, Cooke SJ, Cowley PD, Deng ZD, Fisk AT, et al. Envisioning the future of aquatic animal tracking: technology, science, and application. Bioscience. 2017;67(10):884–96.
25. Lennox RJ, Aarestrup K, Alós J, Arlinghaus R, Aspillaga E, Bertram MG, et al. Positioning aquatic animals with acoustic transmitters. Methods Ecol Evol. 2023;14(10):2514–30.
26. Long M, Jordaan A, Castro-Santos T. Environmental factors influencing detection efficiency of an acoustic telemetry array and consequences for data interpretation. Anim Biotelemetry. 2023;11(1):1–13.
27. Mathies NH, Ogburn MB, McFall G, Fangman S. Environmental interference factors affecting detection range in acoustic telemetry studies using fixed receiver arrays. Mar Ecol Prog Ser. 2014;495:27–38.
28. McCauley DJ, Pinsky ML, Palumbi SR, Estes JA, Joyce FH, Warner RR. Marine defaunation: animal loss in the global ocean. Science. 2015;347(6219):1255641.
29. Melnychuk MC. Detection efficiency in telemetry studies: definitions and evaluation methods. In: Telemetry techniques: a user guide for fisheries research. American Fisheries Society, Bethesda, Maryland, 2012; 339–357.
30. Melnychuk MC, Dunton KJ, Jordaan A, McKown KA, Frisk MG. Informing conservation strategies for the endangered A tlantic sturgeon using acoustic telemetry and multi-state mark–recapture models. J Appl Ecol. 2017;54(3):914–25.
31. Neill SP, Haas KA, Thiébot J, Yang Z. A review of tidal energy—resource, feedbacks, and environmental interactions. J Renew Sustain Energy. 2021;13(6).
32. O'Brien MH, Secor DH. Influence of thermal stratification and storms on acoustic telemetry detection efficiency: a year-long test in the US Southern Mid-Atlantic Bight. Anim Biotelemetry. 2021;9(1):1–12.
33. O'Hara CC, Villaseñor-Derbez JC, Ralph GM, Halpern BS. Mapping status and conservation of global at-risk marine biodiversity. Conserv Lett. 2019;12(4): e12651.
34. O'Hara CC, Frazier M, Halpern BS. At-risk marine biodiversity faces extensive, expanding, and intensifying human impacts. Science. 2021;372(6537):84–7.
35. Olabi AG, Abdelkareem MA. Renewable energy and climate change. Renew Sustain Energy Rev. 2022;158: 112111.
36. Orrell DL, Webber D, Hussey NE. A standardised framework for the design and application of fine-scale acoustic tracking studies in aquatic environments. Mar Ecol Prog Ser. 2023;706:125–51.
37. Pacoureau N, Carlson JK, Kindsvater HK, Rigby CL, Winker H, Simpfendorfer CA, et al. Conservation successes and challenges for wide-ranging sharks and rays. Proc Nat Acad Sci. 2023;120(5): e2216891120.
38. Reubens JT, Pasotti F, Degraer S, Vincx M. Residency, site fidelity and habitat use of Atlantic cod (Gadus morhua) at an offshore wind farm using acoustic telemetry. Mar Environ Res. 2013;90:128–35.
39. Reubens JT, De Rijcke M, Degraer S, Vincx M. Diel variation in feeding and movement patterns of juvenile Atlantic cod at offshore wind farms. J Sea Res. 2014;85:214–21.
40. Reubens J, Verhelst P, van der Knaap I, Deneudt K, Moens T, Hernandez F. Environmental factors influence the detection probability in acoustic telemetry in a marine environment: results from a new setup. Hydrobiologia. 2019;845:81–94.
41. Ripple WJ, Wolf C, Newsome TM, Galetti M, Alamgir M, Crist E, et al. World scientists' warning to humanity: a second notice. Bioscience. 2017;67(12):1026–8.
42. Roy R, Beguin J, Argillier C, Tissot L, Smith F, Smedbol S, De-Oliveira E. Testing the VEMCO Positioning System: spatial distribution of the probability of location and the positioning error in a reservoir. Anim Biotelemetry. 2014;2(1):1–7.
43. Shipley ON, Newton AL, Frisk MG, Henkes GA, LaBelle JS, Camhi MD, et al. Telemetry-validated nitrogen stable isotope clocks identify ocean-to-estuarine habitat shifts in mobile organisms. Methods Ecol Evol. 2021;12(5):897–908.
44. Shipley ON, Manlick PJ, Newton AL, Matich P, Camhi M, Cerrato RM, et al. Energetic consequences of resource use diversity in a marine carnivore. Oecologia. 2022;200(1–2):65–78.
45. Skomal GB, Braun CD, Chisholm JH, Thorrold SR. Movements of the white shark Carcharodon carcharias in the North Atlantic Ocean. Mar Ecol Prog Ser. 2017;580:1–16.
46. Steel AE, Coates JH, Hearn AR, Klimley AP. Performance of an ultrasonic telemetry positioning system under varied environmental conditions. Anim Biotelemetry. 2014;2:1–17.
47. Stenberg C, Støttrup JG, van Deurs M, Berg CW, Dinesen GE, Mosegaard H, et al. Long-term effects of an offshore wind farm in the North Sea on fish communities. Mar Ecol Progr Ser. 2015;528:257–65.
48. Swadling DS, Knott NA, Rees MJ, Pederson H, Adams KR, Taylor MD, Davis AR. Seagrass canopies and the performance of acoustic telemetry: implications for the interpretation of fish movements. Anim Biotelemetry. 2020;8(1):1–12.
49. Tougaard J, Hermannsen L, Madsen PT. How loud is the underwater noise from operating offshore wind turbines? J Acoust Soc Am. 2020;148(5):2885–93.
50. Vemco: Manual on receiver noise measurements. Technical report 2015. https://www.vemco.com/wp-content/uploads/2015/05/receiver-noise.pdf.
51. van der Knaap I, Slabbekoorn H, Winter HV, Moens T, Reubens J. Evaluating receiver contributions to acoustic positional telemetry: a case study on Atlantic cod around wind turbines in the North Sea. Anim Biotelemetry. 2021;9:1–12.
52. van der Knaap I, Reubens J, Thomas L, Ainslie MA, Winter HV, Hubert J, et al. Effects of a seismic survey on movement of free-ranging Atlantic cod. Curr Biol. 2021;31(7):1555–62.
53. van der Knaap I, Slabbekoorn H, Moens T, Van den Eynde D, Reubens J. Effects of pile driving sound on local movement of free-ranging Atlantic cod in the Belgian North Sea. Environ Pollut. 2022;300: 118913.
54. Vergeynst J, Vanwyck T, Baeyens R, De Mulder T, Nopens I, Mouton A, Pauwels I. Acoustic positioning in a reflective environment: going beyond point-by-point algorithms. Anim Biotelemetry. 2020;8:1–17.
55. Wang L, Wang B, Cen W, Xu R, Huang Y, Zhang X, et al. Ecological impacts of the expansion of offshore wind farms on trophic level species of marine food chain. J Environ Sci. 2023;139:226.
56. Wirth C, Warren JD. Spatial and temporal variation in toadfish (Opsanus tau) and cusk eel (Ophidion marginatum) mating choruses in eelgrass (Zostera marina) beds in a shallow, temperate estuary. Bioacoustics. 2020;29(1):61–78.
57. Smith F. Understanding HPE in the Vemco Positioning System (VPS). Halifax, NS: Vemco Inc.; 2013.
58. Meckley TD, Holbrook CM, Wagner CM, Binder TR. An approach for filtering hyperbolicallypositioned underwater acoustic telemetry data with position precision estimates. Animal Biotelemetry, 2014;2:1–13.
59. Wirth C, Warren JD. Spatial and temporal variation in toadfish (Opsanus tau) and cusk eel (Ophidion marginatum) mating choruses in eelgrass (Zostera marina) beds in a shallow, temperate estuary. Bioacoustics, 2020;9(1):61–78.

Publisher's Note